

Expression of DRD2 Is Increased in Human Pancreatic Ductal Adenocarcinoma and Inhibitors Slow Tumor Growth in Mice

1
2
3
4
5
6
7
8
9
10
11
12
13
14
15
16
17
18
19
20
21
22
23
24
25
26
27
28
29
30
31
32
33
34
35
36
37
38
39
40
41
42
43
44
45
46
47
48
49
50
51
52
53
54
55
56
57
58
59
60

Q1 Pouria Jandaghi,^{1,2,3} Hamed S. Najafabadi,^{2,3} Andrea S. Bauer,¹ Andreas I. Papadakis,^{4,5} Matteo Fassan,⁶ Anita Hall,^{5,7} Anie Monast,⁵ Magnus von Knebel Doeberitz,⁸ John P. Neoptolemos,⁹ Eithne Costello,⁹ William Greenhalf,⁹ Aldo Scarpa,^{6,10} Bence Sipos,¹¹ Daniel Auld,^{2,3} Mark Lathrop,^{2,3} Morag Park,^{4,5,12,13} Markus W. Büchler,¹⁴ Oliver Strobel,¹⁴ Thilo Hackert,¹⁴ Nathalia A. Giese,¹⁴ George Zogopoulos,^{5,7} Veena Sangwan,^{5,13} Q2 Sidong Huang,^{4,5} Yasser Riazalhosseini,^{2,3} and Jörg D. Hoheisel¹

1
2
3
4
5
6
7
8
9
10
11
12
13
14
15
16
17
18
19
20
21
22
23
24
25
26
27
28
29
30
31
32
33
34
35
36
37
38
39
40
41
42
43
44
45
46
47
48
49
50
51
52
53
54
55
56
57
58
59
60

¹Functional Genome Analysis, Deutsches Krebsforschungszentrum, Heidelberg, Germany; ²Department of Human Genetics, McGill University, Montreal, Quebec, Canada; ³McGill University and Genome Quebec Innovation Centre, Montreal, Quebec, Canada; ⁴Department of Biochemistry, McGill University, Montreal, Quebec, Canada; ⁵Rosalind and Morris Goodman Cancer Research Centre, McGill University, Montreal, Quebec, Canada; ⁶ARC-NET Center for Applied Research on Cancer, University and Azienda Ospedaliera Universitaria Integrata, Verona, Italy; ⁷The Research Institute of the McGill University Health Centre, Montreal, Quebec, Canada; ⁸Department of Applied Tumor Biology, Institute of Pathology, University Hospital Heidelberg, Heidelberg, Germany; ⁹National Institute for Health Research, Liverpool Pancreas Biomedical Research Unit, Liverpool, UK; ¹⁰Department of Pathology and Diagnostics, Università di Verona, Verona, Italy; ¹¹Institute for Pathology and Neuropathology, Universitätsklinikum Tübingen, Tübingen, Germany; ¹²Department of Pathology, McGill University, Montréal, Quebec, Canada; ¹³Department of Oncology, McGill University, Montréal, Quebec, Canada; and ¹⁴Department of Surgery, University Hospital Heidelberg, Heidelberg, Germany

BACKGROUND & AIMS: Incidence of and mortality from pancreatic ductal adenocarcinoma (PDAC), the most common form of pancreatic cancer, are almost equivalent, so better treatments are needed. We studied gene expression profiles of PDACs and the functions of genes with altered expression to identify new therapeutic targets. **METHODS:** We performed microarray analysis to analyze gene expression profiles of 195 PDAC and 41 non-tumor pancreatic tissue samples. We undertook an extensive analysis of PDAC transcriptome by superimposing interaction networks of proteins encoded by aberrantly expressed genes over signaling pathways associated with PDAC development to identify factors that might alter regulation of these pathways during tumor progression. We performed tissue microarray analysis to verify changes in expression of candidate protein using an independent set of 152 samples (40 nontumor pancreatic tissues, 63 PDAC sections, and 49 chronic pancreatitis samples). We validated the functional relevance of the candidate molecule using RNA interference or pharmacologic inhibitors in pancreatic cancer cell lines and analyses of xenograft tumors in mice. **RESULTS:** In an analysis of 38,276 human genes and loci, we identified 1676 genes that were significantly up-regulated and 1166 genes that were significantly down-regulated in PDAC compared with nontumor pancreatic tissues. One gene that was up-regulated and associated with multiple signaling pathways that are dysregulated in PDAC was G protein subunit $\alpha 2$, which has not been previously associated with PDAC. G protein subunit $\alpha 2$ mediates the effects of dopamine receptor D2 (DRD2) on cyclic adenosine monophosphate signaling; PDAC tissues had a slight but significant increase in *DRD2* messenger RNA. Levels of DRD2 protein were substantially increased in PDACs, compared with non-tumor tissues, in tissue microarray analyses. RNA interference knockdown of DRD2 or inhibition with pharmacologic antagonists (pimozide and haloperidol) reduced proliferation of pancreatic cancer cells, induced endoplasmic

reticulum stress and apoptosis, and reduced cell migration. RNA interference knockdown of DRD2 in pancreatic tumor cells reduced growth of xenograft tumors in mice, and administration of the DRD2 inhibitor haloperidol to mice with orthotopic xenograft tumors reduced final tumor size and metastasis. **CONCLUSIONS:** In gene expression profile analysis of PDAC samples, we found the DRD2 signaling pathway to be activated. Inhibition of DRD2 in pancreatic cancer cells reduced proliferation and migration, and slowed growth of xenograft tumors in mice. DRD2 antagonists routinely used for management of schizophrenia might be tested in patients with pancreatic cancer.

Keywords: TMA; Unfolded Protein Response; Drug Repositioning; Pancreas.

The overall 5-year survival rate of all cancer patients stands at 63%, and only about 5% for pancreatic cancer—a number that has remained largely unchanged for the last 3 decades.¹ Of the patients diagnosed with pancreatic cancer, approximately 85% exhibit pancreatic

Abbreviations used in this paper: cAMP, cyclic adenosine monophosphate; CP, chronic pancreatitis; CSC, cancer stem cells; DMSO, dimethylsulfoxide; DRD2, dopamine receptor D2; ER, endoplasmic reticulum; FDA, Food and Drug Administration; GNAI2, guanine nucleotide binding protein α inhibiting activity polypeptide 2; GPCR, G-protein-coupled receptors; PDAC, pancreatic ductal adenocarcinoma; PKA, protein kinase A; shRNA, short hairpin RNA; UPR, unfolded protein response.

© 2016 by the AGA Institute
0016-5085/\$36.00

<http://dx.doi.org/10.1053/j.gastro.2016.08.040>

ductal adenocarcinoma (PDAC); most of them die within 6 months after diagnosis. The poor prognosis is caused by a lack of apparent symptoms early during the disease and consequently its detection at only late stages. This goes along with an aggressive tumor biology, in particular, very early metastasis. Finally, effective options for chemotherapy are lacking.² The widely used chemotherapeutic agent gemcitabine confers a median survival advantage of only 6 months,³ also because the vast majority of patients develop resistance to therapy.⁴ Given this poor prospect, there is an urgent need for effective treatment modalities. To this end, we set out to investigate potential therapeutic targets by dissecting gene expression profiles of tumors and control samples. Candidate targets were validated with respect to their suitability and analyzed functionally. Using this approach, dopamine receptor D2 (DRD2) was found as a novel, promising protein for the development of a targeted therapy. We show that DRD2 has a central role in proliferation and survival of pancreatic cancer cells. Pharmacologic blockade of DRD2 activity with inhibitors, including the Food and Drug Administration (FDA)-approved DRD2 antagonists pimozone and haloperidol, suppressed the proliferation of pancreatic cancer cells, while having a markedly attenuated effect on normal fibroblasts. Further functional assays demonstrated substantial effects on migration, cell cycle progression and apoptosis as well, providing a broad therapeutic spectrum, and revealed the pathways and mechanisms involved in these processes.

Material and Methods

Detailed information describing methods used in each of the following sections are provided in the [Supplementary Material](#).

Tissue RNA Profiling

The study was performed with tissue samples obtained from patients admitted to the Department of General, Visceral and Transplantation Surgery, University of Heidelberg and the National Institute for Health Research, Liverpool. The study was conducted in accordance with the Helsinki Declaration; written informed consent was obtained from all patients; ethical approval was obtained from the ethical committee of the University of Heidelberg (case number 301/2001). Total RNA from individual samples was analyzed on the Sentrix Human-6v3 Whole Genome Expression BeadChips (Sentrix Human WG-6; Illumina) as suggested by the manufacturer. Information about clinical annotations of samples, isolation of RNA, and microarray expression data analysis, as well as downstream pathway and network analysis, are provided in [Supplementary Table 1](#) and [Supplementary Material](#).

Cell Lines and Reagents

Five pancreatic cancer cell lines with various degree of differentiation were obtained from the American Type Culture Collection (Manassas, VA). The moderately differentiated BxPC-3 cells, as well as the poorly differentiated cell lines Panc-1 and MiaPaCa-2, originated from primary tumor. The

well-differentiated cell lines Capan-1 and CFPAC-1 were isolated from liver metastases of pancreas adenocarcinoma. Normal human dermal fibroblasts were obtained from PromoCell (Heidelberg, Germany). Pimozide, L-741,626, haloperidol, thapsigargin, SQ22536, and H-89 were purchased from Sigma-Aldrich (Munich, Germany).

Plasmids and Viral Transduction

All lentiviral short hairpin RNA (shRNA) vectors were obtained from the Mission TRC genome-wide shRNA collection of Sigma-Aldrich. Additional information about the shRNA vectors can be found at http://www.broad.mit.edu/genome_bio/trc/rnai.html using the TRCN number. The following lentiviral shRNA vectors targeting *DRD2* or *ATF4* were used: TRCN0000011342 (shDRD2#1), TRCN0000011343 (shDRD2#2), TRCN0000013573 (shATF4#1), and TRCN0000013575 (shATF4#2). Vector pLKO.1 was used as negative control. Lentivirus production is described in the [Supplementary Material](#).

Quantitative Real-Time Polymerase Chain Reaction

For mice xenograft tissue samples and cultured cells, the miRNeasy kit (Qiagen, Valencia, CA) was used to extract total RNA. Reverse transcription was done using the Maxima First Strand cDNA Synthesis Kit for RT-qPCR (Thermo Scientific Rockford, Logan, UT). Real-time polymerase chain reaction was run using the ViiA 7 Real-Time PCR System (Applied Biosystems, Darmstadt, Germany) and the FastStart Universal SYBR Green Master Mix (Roche Diagnostics, Mannheim, Germany) according to the manufacturers' specifications. Relative messenger RNA levels of *DRD2* were normalized to the expression of the housekeeping gene glyceraldehyde 3-phosphate dehydrogenase. Quantification values were calculated according to a standard curve method created from a dilution series. Polymerase chain reactions were performed in triplicate.

Western Blot Analysis

Western blot analysis was performed as described previously.⁵ Detailed procedure and antibodies are described in the [Supplementary Material](#).

Colony-Formation Assay

Single-cell suspensions of the indicated parental or transduced pancreatic cancer cell lines were plated in 6-well plates ($2-4 \times 10^4$ cells/well), and were cultured for 12-15 days while growth medium was refreshed every 4 days. Cells were then washed with phosphate-buffered saline, fixed with paraformaldehyde, stained with crystal violet (0.1% w/v; Sigma-Aldrich) and photographed. Assays were performed independently at least 3 times.

Measurement of the Free Ca^{2+} Concentration in Cytosol

Intracellular Ca^{2+} levels were measured using the Fluo-4 NW Calcium Assay Kit (Invitrogen, Karlsruhe, Germany) according to the manufacturer's protocol.

Fluorescence-Activated Cell Sorting Cell Cycle Analysis

Cancer cells were plated into the wells of 12-well plates (NUNC, Roskilde, Denmark) and allowed to grow for 24 hours. Drug treatment was performed for 48 hours with different concentrations. Cells were harvested by trypsinization and washed with cold phosphate-buffered saline. Cold Nicoletti buffer was used for staining and the DNA content of single nuclei was analyzed by flow cytometry on a FACSCANTO II analyzer (BD Biosciences, Heidelberg, Germany) with collection of at least 10,000 events for each sample and in 3 independent experimental repetitions.

Cell Viability

Sulforhodamine B sodium salt (Sigma-Aldrich) assay was used to assess cell viability.

Caspase 3/7 Activity

The cell apoptosis caused by DRD2 antagonists was determined using the Caspase-Glo 3/7 Assay kit (Promega, Madison, WI) according to the manufacturer's instructions.

In Vivo Experiments

Severe combined immunodeficient beige mice were bred in-house. One million Panc-1 cell transduced with shDRD2#1, shDRD2#2, or pLKO were suspended in 150 μ L phosphate-buffered saline and mixed with 150 μ L Matrigel (BD Biosciences, San Jose, CA) before the respective suspension was injected subcutaneously into the left and right flank of a mouse. For each test cell line, 3 mice were injected with cells in both flanks. Tumor size was determined twice a week using a caliper to measure the volume of the tumor according to the formula: volume (V) = length (L) \times depth (D) \times width (W). After reaching the appropriate volume, primary tumors were resected. In case of pLKO, this happened on day 51 after injection; for shDRD2#1 and shDRD2#2 the tumor was removed after 65 days. Tumors were embedded in paraffin after zinc fixation for immunohistochemistry and H&E staining, or stored at -80°C for RNA extraction.

Two million MIAPaCa-2 cells resuspended in 10 μ L Matrigel (BD Biosciences, San Jose, CA) were orthotopically implanted into the tail of the pancreas of 6-week-old Nod scid gamma animals (Jackson Labs, Bar Harbor, ME) (day 1). When tumors were palpable (day 27), mice were randomized into 2 groups ($n = 7$ in control group and $n = 9$ in haloperidol group) and injected intraperitoneally with either haloperidol (10 mg/kg) or solvent (dimethylsulfoxide [DMSO] control group) for 12 days. The experiment was terminated when control mice appeared moribund. Weight of the animal and final tumor weight and volume were measured. The studies were approved by the Animal Care Committee of McGill University Faculty of Medicine.

Statistical Analysis

GraphPad Software 6 for Windows (GraphPad, San Diego, CA), SigmaPlot 12.5 (Systat Software, San Jose, CA) and Microsoft Excel 2010 (Redmond, WA) were used for statistical analysis and graph creation. Data are presented as mean SE from 3–8 independent experiments, depending on the

assay. An analysis of difference between the mean of 2 data sets was carried out using the nonparametric Mann-Whitney U test. P values $<.05$ were considered as statistically significant.

Results

Gene Expression Profiling Identifies Pancreatic Ductal Adenocarcinoma–Associated Pathways

We examined the expression profiles of 38,276 human genes and loci across pancreatic tissue samples from 195 PDAC patients and 41 healthy control subjects (Table 1 and Supplementary Table 1; the complete data set is accessible at the public ArrayExpress database [E-MTAB-1791]). This analysis revealed widespread deregulation of gene expression in PDAC, including 1676 and 1166 genes that were substantially up- or down-regulated in PDAC, respectively (false discovery rate <0.01 , Supplementary Table 2). Interestingly, we found that many up-regulated genes were associated with several cancer-related pathways according to the *Kyoto Encyclopedia of Genes and Genomes*⁶ data sets, with the most significant association corresponding to “pathways in cancer” ($P < 5 \times 10^{-9}$; Figure 1A and Supplementary Table 3). Many of the genes associated with “pathways in cancer” were also linked to other PDAC-enriched processes (Figure 1B), suggesting a central role for these “multipathway” genes as potential functional hubs contributing to PDAC. This was further supported by several previous studies that reported a connection between these genes and pancreatic cancer (Figure 1B and Supplementary Table 4), highlighting the notion that many of these multipathway genes are reproducibly linked to PDAC.

One of the PDAC-related multipathway genes was guanine nucleotide binding protein α inhibiting activity

Table 1. Characteristics of the Patients Whose Tumors Were Analyzed by Gene Expression Profiling

Characteristic	Samples (n = 195)
Sex, n (%)	
Female	86 (44.1)
Male	109 (55.9)
Stage, n (%)	
0	0
IA	1 (0.5)
IB	0
IIA	20 (10.2)
IIB	116 (59.4)
III	15 (7.6)
IV	19 (9.7)
NA	24 (12.3)
Tumor grade, n (%)	
1	2 (1.0)
2	106 (54.3)
3	60 (30.7)
4	0
NA	27 (13.8)
Age, y, median (range)	68 (43–88)

NA, XX.

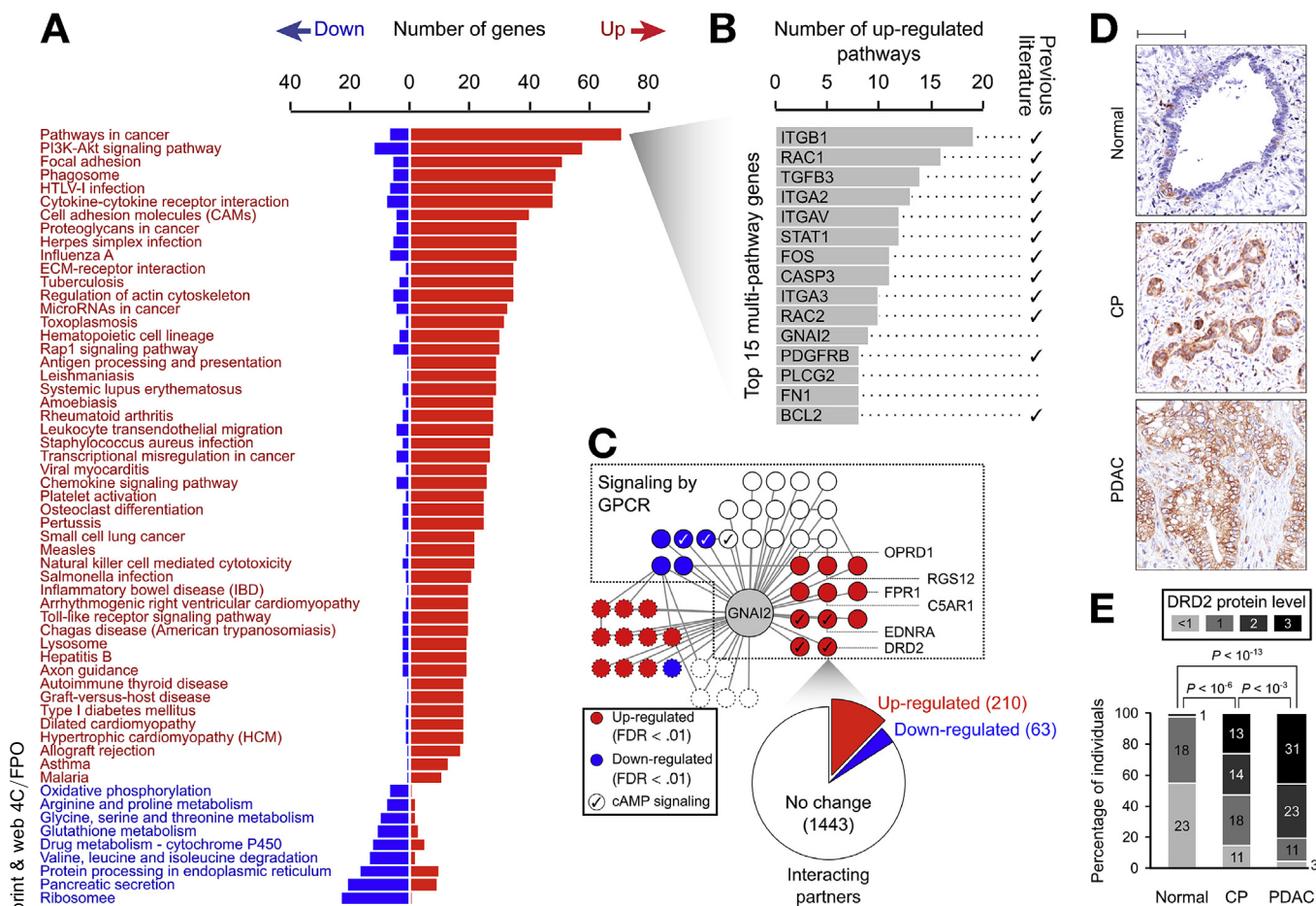


Figure 1. Gene expression analysis. (A) Pathways or functions that are significantly up- or down-regulated in the PDAC transcriptome are shown in red and blue, respectively (false discovery rate [FDR] <0.025). The number of significantly de-regulated genes of each pathway (FDR <0.01, fold-change >1.5) is shown on the right. (B) Top 15 multipathway genes of the “pathways in cancer” annotation. For each gene, the total number of up-regulated PDAC pathways is indicated. Genes that were previously reported to have association with pancreatic cancer, or to have a pancreatic cancer-associated homolog, are marked (see Supplementary Table 4 for a list of publications related to each gene). (C) GNAI2, as the top multipathway candidate for pancreatic cancer that has not been previously implicated, directly interacts with several other PDAC de-regulated proteins, the majority of which are also up-regulated. Most interactions are with other components of the GPCR signaling pathway. Among the up-regulated interacting partners in this signaling pathway, DRD2 is an aberration hub, with a significant proportion of its first and second-degree neighbors being up-regulated in PDAC samples. Other aberration hubs are also identified by their names. (D) Immunohistochemical analysis of DRD2 protein levels in PDAC samples on tissue micro-arrays. Representative examples of DRD2 expression in duct cells of normal pancreas, CP and PDAC are shown. Normal ductal cells were almost DRD2-negative or showed a mild positivity in pancreatic ducts. CP lesions and PDACs represented moderate/strong and strong DRD2 expression, respectively. Sizing bar indicates 100 μ m. (E) The staining intensity was categorized into 4 groups: <1 = no or poor staining (negative); 1 = weak staining; 2 = moderate staining; and 3 = strong staining. The distribution of DRD2 expression in the clinical tissue samples revealed its high expression in PDAC ($P < 10^{-13}$) and CP ($P < 10^{-6}$) as compared with normal tissues. P values were calculated by Student t test.

polypeptide 2 (*GNAI2*). Surprisingly, we did not find any previous report about a connection of *GNAI2* and pancreatic cancer, despite its clear up-regulation in PDAC ($P < 3 \times 10^{-12}$, fold-change >2) and its association with 9 PDAC-related pathways. *GNAI2* is an α subunit of the guanine nucleotide-binding proteins (G proteins) and primarily functions in G-protein coupled receptor (GPCR) signaling by regulation of adenylate cyclase.⁷ In addition, we observed that *GNAI2* interacts with several genes that were up-regulated in PDAC, particularly other proteins of the GPCR and cyclic adenosine monophosphate (cAMP pathways) (Figure 1C),

further supporting its role as a functional signaling hub in PDAC.

GNAI2 Interacting Partner Dopamine Receptor D2 Is Up-Regulated in Pancreatic Ductal Adenocarcinoma

GNAI2 couples cell surface receptors to intracellular pathways, primarily to cAMP signaling.⁸ In order to identify cell surface receptors that may take advantage of *GNAI2* up-regulation to exert their oncogenic activities in PDAC, we

systematically looked for “aberration hubs” among the interacting partners of GNAI2 that were up-regulated in PDAC. An aberration hub is defined as a protein that exhibits an unexpectedly large number of physical or functional interactions with “aberrant” proteins; in this case proteins that are significantly up-regulated in PDAC (see Materials and Methods). Aberration hubs often highlight proteins that are central in disease modules.⁹ We identified 6 significant aberration hubs among the interacting partners of GNAI2 that are involved in GPCR signaling (false discovery rate <0.01, Figure 1C). One of them is DRD2, which uses GNAI2 to regulate the cAMP-signaling pathway, the deregulation of which is intrinsic to pancreatic cancer.¹⁰ However, in PDAC samples, the microarray analysis only identified a slight, although very significant, increase in *DRD2* messenger RNA

levels (1.08-fold; $P < .0002$). This initially suggested that low levels of DRD2 could act as a bottleneck in this pathway, therefore, limiting the effect of GNAI2 up-regulation. However, tissue microarray analysis of DRD2 across 40 normal pancreatic tissues, 63 PDAC sections, and 49 samples of chronic pancreatitis (CP), an inflammation of the pancreas associated with high risk of PDAC¹¹ (Supplementary Table 5), revealed that DRD2 protein levels were significantly increased in PDAC and CP compared with normal samples (>3-fold), with the highest level detected in PDAC (>4-fold, $P < 10^{-13}$, Figure 1D and E). These results mirrored up-regulation of *GNAI2* in PDAC and suggested that DRD2 up-regulation, most likely due to a post-transcriptional aberration, may contribute to malignancy.

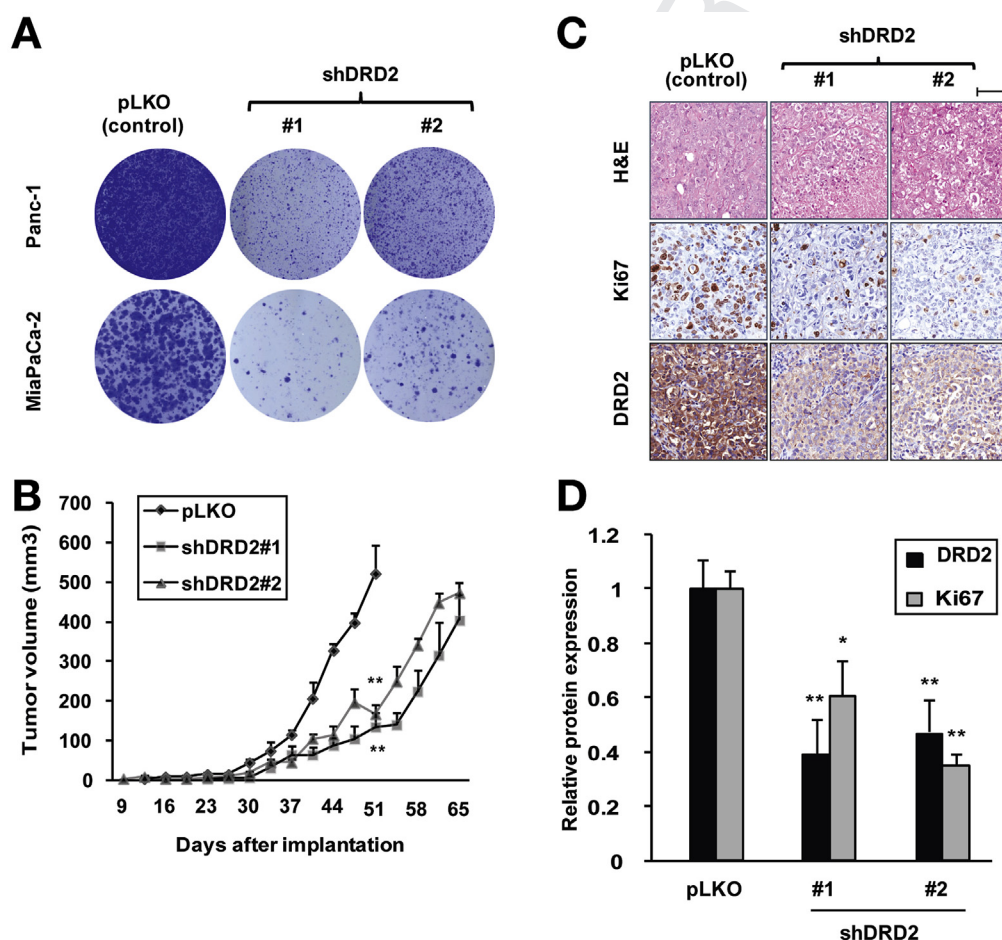
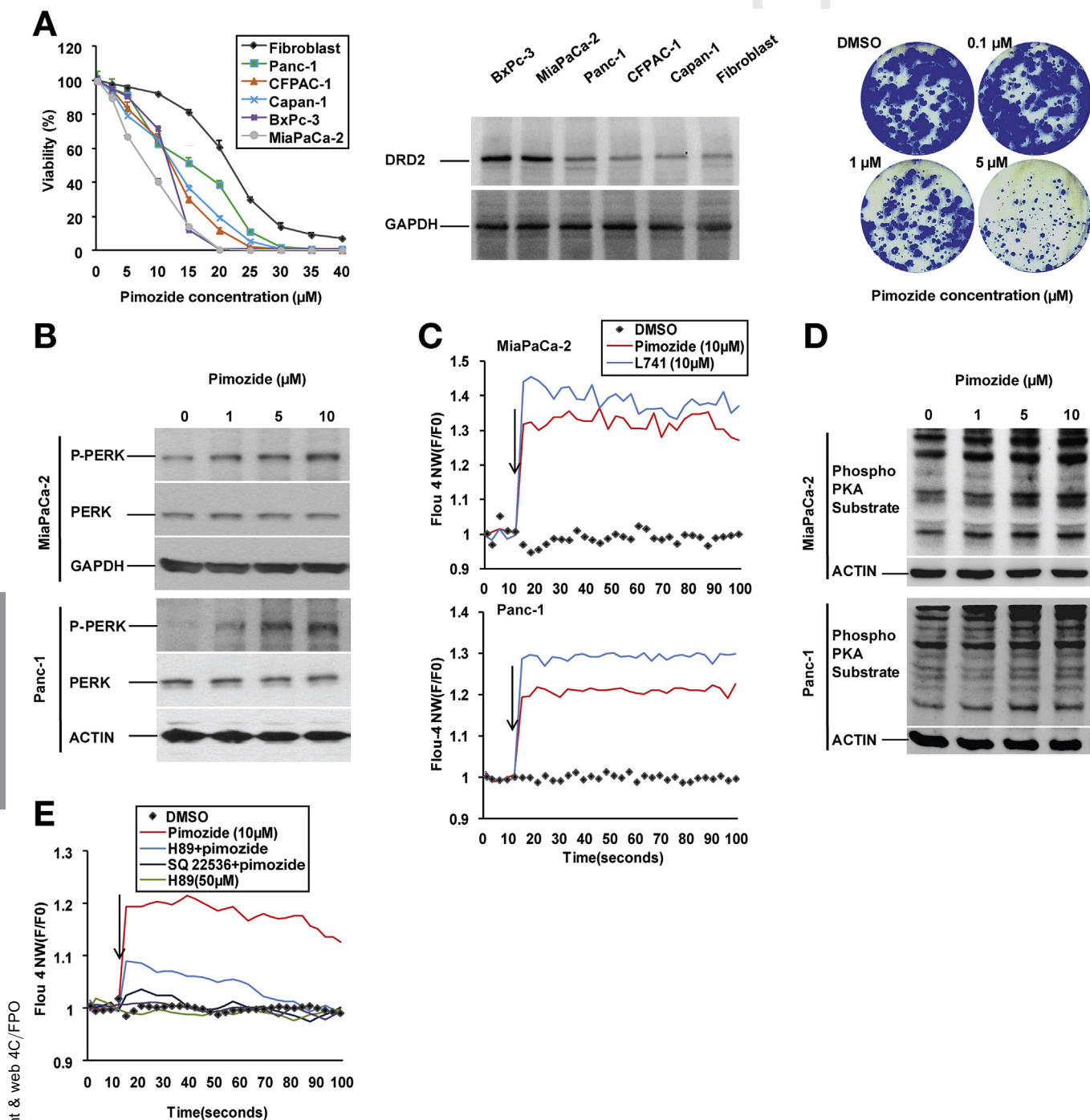


Figure 2. Silencing of *DRD2* inhibits cancer cell growth in vitro and in vivo. (A) Colony-formation assay with MiaPaCa-2 and Panc-1 cells infected with the lentiviral vector pLKO as a control or constructs expressing 1 of 2 independent shRNAs targeting *DRD2* (shDRD2#1 and #2). The cells were fixed, stained, and photographed after 12 days. The efficacy of knockdown was assessed by quantitative reverse transcription polymerase chain reaction (Supplementary Figure 1A). (B) Tumor growth was monitored by measuring tumor volume in mice implanted with Panc-1 cells expressing the negative control (pLKO) or shDRD2 (3 mice per group, each implanted with cells in both flanks). There was a significant decrease in tumor growth in mice implanted with DRD2-deficient cells ($P = .002$). (C) Representative figures of histologic examination of the tumors procured from mice. H&E staining did not show any pathologic difference in DRD2-deficient tumors compared with controls, with the exception of cell ballooning in some areas of a tumor generated from cells infected with shDRD2#2. Staining for Ki-67, a marker of cell proliferation confirmed decreased proliferation in DRD2-deficient cells. Analysis with an antibody against DRD2 confirmed the efficacy of knockdown. Sizing bar indicates 50 μm . (D) Bar plots summarizing the immunohistochemistry results described in (C) for all tumors ($n = 18$). Data are presented as mean \pm SE throughout the figure. * $P < .05$ and ** $P < .01$ when compared with the corresponding results from pLKO-infected cells (Mann-Whitney U test).

Silencing of Dopamine Receptor D2 Inhibits Cancer Cell Growth *In Vitro* and *In Vivo*

To determine whether DRD2 contributes to tumor cell growth and survival, we suppressed DRD2 expression in the pancreatic cancer cell lines Panc-1 and MiaPaCa-2 through lentiviral delivery of expression vectors of shRNAs targeting *DRD2*. Knockdown of *DRD2* expression by 2 independent shRNA constructs impaired proliferation of both cell lines as measured by a long-term colony-formation assay (Figure 2A and Supplementary Figure 1A).

For confirmation *in vivo*, we subcutaneously injected 1×10^6 Panc-1 cells expressing either of the 2 shRNAs targeting *DRD2* or the pLKO control into severe combined immunodeficient beige mice, with 2 replicates, and monitored tumor size over time. Mice implanted with pLKO-expressing cells developed tumors much earlier (21.7 ± 1.6 days) than those engrafted with DRD2-deficient cells (33.3 ± 1.2 days with shDRD2#1 or 27.2 ± 1.5 days with shDRD2#2). Mice engrafted with DRD2-deficient cells exhibited significantly reduced tumor volume compared



with the control group ($P < .002$, Figure 2B), while there was no significant difference in body weight between control and test groups (Supplementary Figure 1B). Immunohistochemical analysis of the tumors confirmed the reduced levels of DRD2 in tissues isolated from animals treated with DRD2-deficient cells compared with the controls (Figure 2C and D), in line with lower DRD2 messenger RNA levels in tumors developed from DRD2-deficient cells as assayed by quantitative reverse transcription polymerase chain reaction (Supplementary Figure 1C). Concomitant to the reduction in DRD2, protein Ki-67—a marker of cell proliferation¹²—was markedly reduced (Figure 2C and D). These results demonstrated that DRD2 has a key role in proliferation and survival of tumor cells.

Pharmacologic Blockade of Dopamine Receptor D2 Impairs Cancer Cell Growth

We examined the effect of pharmacologic inhibition of DRD2 on cancer cell proliferation. Different concentrations of the DRD2 antagonist pimoizide, an FDA-approved DRD2 inhibitor used for treatment of schizophrenia,¹³ were tested on 5 established pancreatic cancer cell lines—Panc-1, CFPAC-1, Capan-1, MiaPaCa-2, and BxPC-3. Treatment with pimoizide resulted in a dose-dependent inhibitory effect on cell growth in all examined cell lines. Notably, the pimoizide effect was stronger in MiaPaCa-2 and BxPC-3 cells, which showed higher expression levels of DRD2 among the cell lines, and weaker on a primary normal fibroblast cell line used as a control (Figure 3A). We repeated the assay with another DRD2 inhibitor, L-741,626 (L-741).¹⁴ L-741 treatment had virtually the same effect (Supplementary Figure 2A). Taken together, our results demonstrated that pharmacologic blockade of DRD2 activity inhibits proliferation of pancreatic cancer cells.

Induction of Endoplasmic Reticulum Stress in Response to Dopamine Receptor D2 Blockade

Deficiency of DRD2 leads to endoplasmic reticulum (ER) stress,¹⁵ the severe form of which has anti-proliferative and pro-apoptotic effects in cancer cells.¹⁶ We examined the

possible effect of DRD2 blockade on induction of ER stress by evaluating the level of phosphorylated PERK (Thr 981). Pimoizide increased phosphorylation of PERK in a dose-dependent manner in both Panc-1 and MiaPaCa-2 cells, as determined by immunoblotting (Figure 3B). Similar results were obtained by treating cells with L-741 (Supplementary Figure 2B). As ER stress is coupled to the release of Ca^{2+} from the ER into the cytosol,¹⁷ we examined whether DRD2 inhibition would affect the cytosolic abundance of Ca^{2+} . Indeed, treatment with both pimoizide and L-741 increased the concentration of cytosolic Ca^{2+} within seconds in Panc-1 and MiaPaCa-2 (Figure 3C), showing that DRD2 blockade induces ER stress in PDAC cells.

Cyclic Adenosine Monophosphate and Protein Kinase A Mediates the Effects of Dopamine Receptor D2 Inhibition on Endoplasmic Reticulum Stress

It has been shown that cAMP and protein kinase A (PKA) regulate Ca^{2+} levels in the cytosol and are involved in ER stress.^{18,19} It has also been reported that DRD2 modulates intracellular cAMP formation.²⁰ Accordingly, we examined whether induction of ER stress by DRD2 blockade would be mediated by cAMP and PKA. To this end, the activity of PKA, which is dependent on the presence of cAMP, was measured through Western blot analysis using a phospho-PKA substrate antibody in Panc-1 and MiaPaCa-2 cells following treatment with pimoizide. Activation of PKA was detected upon incubation with 1 μ M pimoizide. The effect grew stronger with the administration of higher drug concentrations (Figure 3D), indicating that cAMP/PKA is activated in a dose-dependent manner upon inhibition of DRD2.

In order to examine whether the ER stress induced by DRD2 inhibition is influenced by modulation of cAMP or PKA, Panc-1 cells were pretreated with SQ22536, a specific cAMP inhibitor, to down-regulate cAMP and PKA activation; alternatively, the drug H-89²¹ was used to block PKA. Strikingly, the pimoizide-induced release of Ca^{2+} from the ER to cytoplasm was completely blocked or substantially reduced by a pretreatment with SQ22536 or H-89,

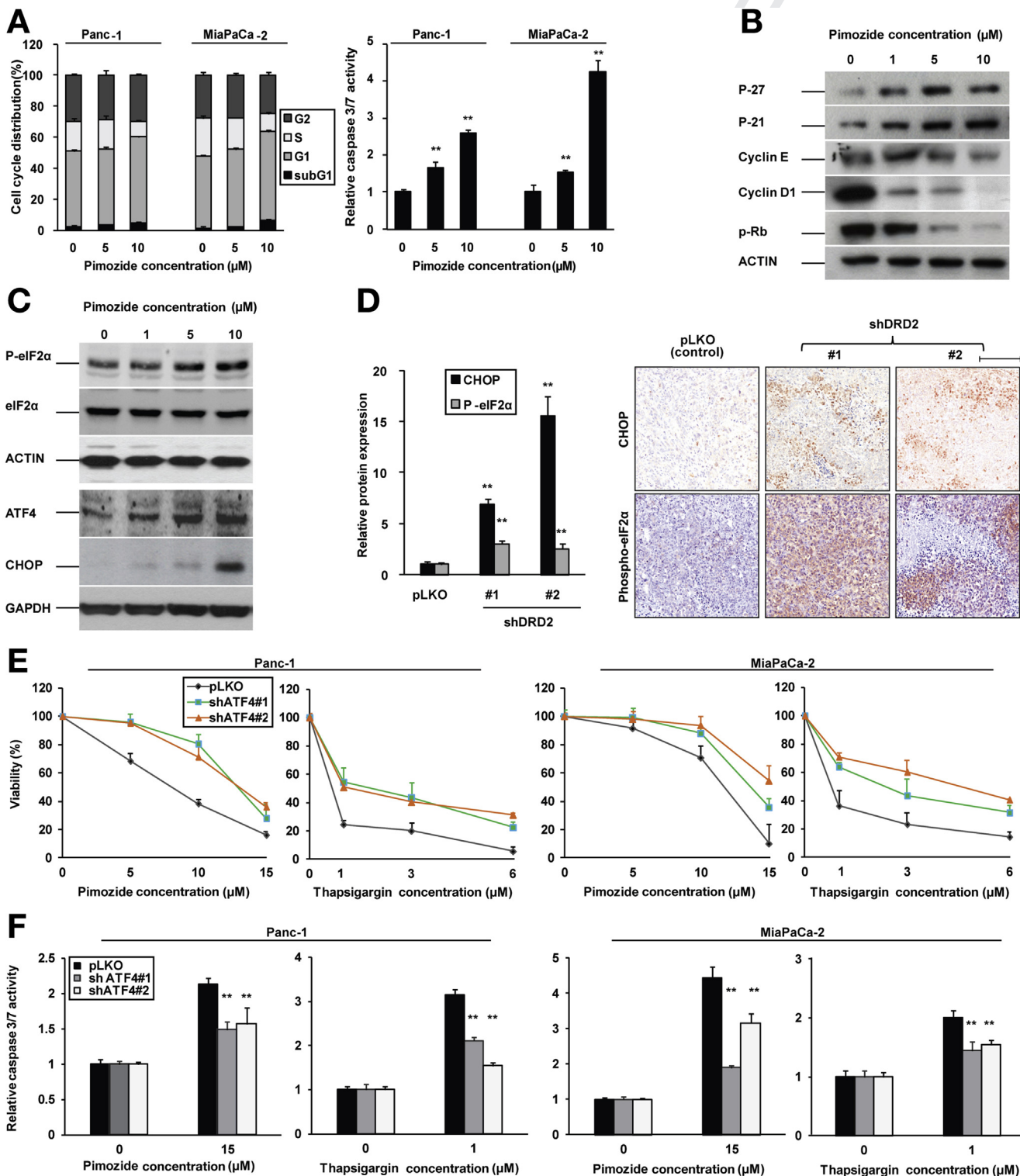
Figure 3. Pharmacologic blockade of DRD2 reduces cell viability in PDAC cells. (A) Left: Panc-1, CFPAC-1, Capan-1, MiaPaCa-2, BxPC-3, and fibroblast cells were seeded for 24 hours and subsequently exposed to various concentrations of pimoizide for 72 hours. Cell viability was determined using the sulforhodamine B assay. Values are the mean \pm SD of 6 independent experiments. Middle: DRD2 levels in the cell lines assayed by Western blot. Right: Effect of long-term (15 days) treatment with increasing doses of pimoizide on colony-forming ability of Panc-1. (B) The effect of pimoizide on the activation of ER stress in MiaPaCa-2 (top) and Panc-1 (bottom) cells. Cells were seeded for 24 hours and then treated with different doses of pimoizide for 2 hours. Protein was extracted and equal amounts of cell lysates were analyzed by WB using ER stress indicator antibodies PERK and p-PERK. (C) Effect of pimoizide and L741 on Ca^{2+} release from ER to cytoplasm in MiaPaCa-2 (top) and Panc-1 (bottom) cells. Cells were treated with the Fluo-4 dye 24 hours after seeding and baseline values were recorded for 10 seconds. Then, Pimoizide, L741 or DMSO was added. Fluorescence was measured for 90 seconds and the mean of 3 independent assays was normalized to their baselines. (D) Dose dependent induction of PKA activity by pimoizide in MiaPaCa-2 (top) and Panc-1 (bottom) cells. Cells were seeded for 24 hours and subsequently treated with pimoizide for 2 hours. Total protein was extracted and equal amounts of cell lysates were analyzed by Western blot analysis using a phospho-PKA substrate antibody. (E) Inhibition of PKA by SQ22536 and H-89 rescued the ER stress induced by pimoizide, documented by a reduced release of Ca^{2+} from the ER to the cytoplasm. Panc-1 cells were seeded for 24 hours and treated with the Fluo-4 dye; baseline values were recorded for 10 seconds after pretreatment with SQ 22536 and H-89. Then, cells were treated with pimoizide or DMSO. Fluorescence was measured for 100 seconds and the mean of 3 independent assays were normalized to their baseline values.

respectively (Figure 3E). The stronger reduction of Ca²⁺ levels by SQ22536 may be explained by the finding that cAMP affects all calcium transport system receptors in the ER, whether they are PKA-dependent or not.¹⁸ Together, our findings showed that DRD2 antagonists increase cytosolic levels of Ca²⁺ in a rapid and effective manner; the level of cAMP, which acts downstream of DRD2,^{22,23} is increased after the blockade of DRD2; and Ca²⁺ levels are

positively regulated by cAMP mainly and to a lesser extent by PKA.

Dopamine Receptor D2 Blockade Impairs Cell Cycle Progression and Induces Apoptosis

Previous studies have shown that ER stress can affect the cell cycle at the G1/S transition via regulating cyclin D1.^{24,25} We therefore investigated the effect of DRD2



inhibition on cell cycle progression. Panc-1 and MiaPaCa-2 cells were treated with different concentrations of Pimozide for 48 hours and their distribution in the cell cycle states was analyzed using fluorescence-activated cell sorting. Pimozide-induced cell cycle arrest at the G1 phase in a dose-dependent manner (Figure 4A). In addition, the increase in the fraction of cells in sub-G1 in the fluorescence-activated cell sorting analysis indicated a higher number of apoptotic cells. To verify this, activation of caspase 3/7 was examined 24 hours post-treatment with pimozide. Caspase 3/7 activity grew with increasing pimozide concentrations (Figure 4A), confirming that inhibition of DRD2 induces apoptosis in PDAC cells.

We further validated the induction of cell cycle arrest at a molecular level by measuring the abundance of cell cycle checkpoint proteins. Consistent with the fluorescence-activated cell sorting data, Western blot analysis showed a decrease in the cyclin D1, p-Rb, and cyclin E1 levels, and an increase in the levels of p21 and p27 in a dose-dependent manner, confirming G1 cell cycle arrest (Figure 4B).

Dopamine Receptor D2 Inhibition Activates Unfolded Protein Response in Pancreatic Cancer Cells

As reported here, the blockade of DRD2 led to phosphorylation and thus activation of PERK, which is a marker of unfolded protein response (UPR). Recent studies have shown that a strong induction of UPR as indicated by PERK activation can lead to UPR-induced apoptosis through phosphorylation of downstream molecule eIF2 α and selective induction of ATF4, which in turn increases the expression of CHOP.²⁶ Therefore, we examined the activity and expression levels of proteins involved in the PERK arm of UPR after treatment of cells with pimozide (Figure 4C). Phosphorylation of eIF2 α as well as the expression levels of ATF4 and CHOP increased upon pimozide treatment in a dose-dependent manner, in line with the increase in activated PERK (Figure 3B). We further investigated the induction of UPR in DRD2-deficient cells in vivo. In severe combined immunodeficient beige mice, the abundance of

phosphorylated eIF2 α (p-eIF2 α) and CHOP was assessed in tumors that developed after implantation of Panc-1 cells infected with shDRD2 constructs or the pLKO control. Immunohistochemical analysis on tumor samples demonstrated the elevated levels of p-eIF2 α and CHOP in tumors developed from DRD2-deficient cells as compared with the control tumors (Figure 4D). These findings provide evidence that inhibition of DRD2 triggers UPR. To investigate the extent to which activation of ER-UPR signaling mediates growth inhibitory function of DRD2 blockade, we generated ATF4-deficient sublines of Panc-1 and MiaPaca-2 cells through stable knock-down using 2 specific ATF4-shRNAs (Supplementary Figure 3A and B), and examined effects of DRD2 inhibition in these models. Likewise, we tested effects of the ER stress inducer, thapsigargin,²⁷ on cell viability and apoptosis in these cells. Reduction of cell viability and induction of apoptosis after treatment with pimozide or thapsigargin were significantly declined in ATF4-deficient cells compared with control (pLKO) (Figure 4E and F). Similar results were obtained after treatment of these cells with L-741 (Supplementary Figure 3C–F). These results show that the UPR pathway is an important mediator of growth inhibitory effects of DRD2 blockade.

Blockade of Dopamine Receptor D2 Inhibits Cancer Cell Migration

Our previous results showed that DRD2 regulates the cAMP level, which is known to modulate cell adhesion and motility in pancreatic cancer cells.¹⁰ Consequently, we studied whether DRD2 inhibition has an effect on cancer cell migration by assessing the motility of the highly invasive Panc-1 cells in a wound healing assay in the presence of the DRD2 antagonists pimozide and L-741. Both antagonists reduced migration of Panc-1 cells in a dose-dependent manner using concentrations that did not inhibit cell growth (Figure 5A and Supplementary Figure 4A and B). Consistent with this result, we observed a gradual rise in the expression of E-cadherin protein and a simultaneous decrease in vimentin levels (Figure 5B). To exclude the possibility that the effect of DRD2 inhibition on cell

Figure 4. Pimozide induces apoptosis and cell cycle arrest at G1 phase in PDAC cells. (A) *Left:* Panc-1 and MiaPaCa-2 cells were seeded for 24 hours and treated with increasing concentrations of pimozide or DMSO for 48 hours. Cells were fixed and stained with Nicoletti buffer, and cell cycle distribution was analyzed by fluorescence-activated cell sorting. Sub-G1 and G1 cells increased with increasing pimozide concentrations in both Panc-1 ($P < .003$ and $< .001$ for sub-G1 and G1, respectively) and MiaPaCa-2 cells ($P < 7 \times 10^{-4}$ and $< 4 \times 10^{-5}$ for sub-G1 and G1, respectively). Conversely, S-phase cells decreased with higher pimozide concentrations in both Panc-1 and MiaPaCa-2 ($P < .003$ and $< 3 \times 10^{-5}$, respectively; all P values are obtained by regression slope t test). *Right:* Dose-dependent activation of caspase 3/7 in PDAC cells after treatment with pimozide. Panc-1 and MiaPaCa-2 were exposed to pimozide and DMSO as control for 24 hours. Then, caspase 3/7 activity was measured. (B) The effect of pimozide on cell cycle checkpoint proteins. Total protein was extracted from Panc-1 cells treated with pimozide. Equal amounts of cell lysate were analyzed by Western blot using antibodies against each protein. (C) Pimozide activates the PERK signaling cascade of UPR. Phosphorylation of eIF2 α and expression levels of ATF4 and CHOP were assayed by Western blot analysis after 2-hour and 24-hour treatment with pimozide in Panc-1 cells, respectively. (D) Silencing of DRD2 induces the PERK signaling cascade of UPR in tumors of xenograft mice. *Left:* Knockdown of DRD2 led to increased levels of CHOP and P-eIF2 α as assayed by immunohistochemistry (IHC). *Right:* Representative images of IHC analysis are shown. Inhibition of ER stress-UPR activation through ATF4 knockdown rescues, at least in part, the anti-proliferative (E) and apoptosis-inducing (F) effects of pimozide on Panc-1 and MiaPaca-2 cells. The ER stress inducer, thapsigargin, serves as a positive control. ** $P < .01$ when compared with the corresponding results at 0 μ M or pLKO condition (Mann-Whitney U test).

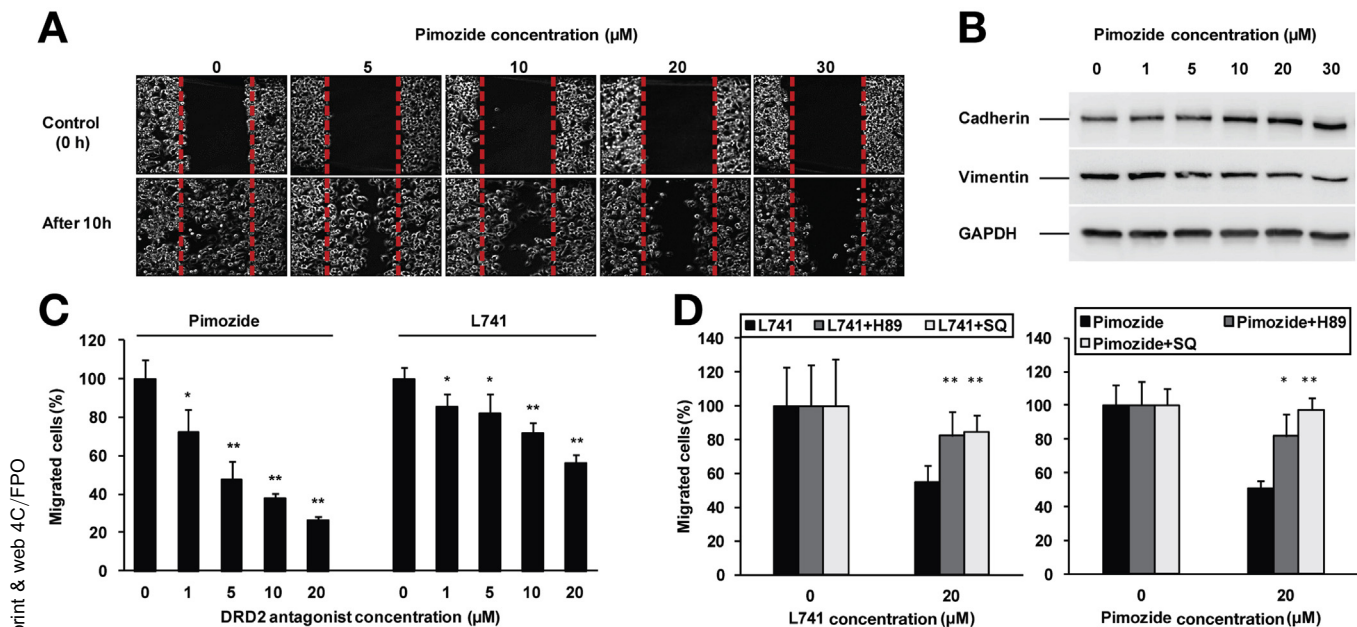


Figure 5. Inhibitory effect of DRD2 blockade on migration of pancreatic cancer cells. (A) A wound was made in the confluent monolayer culture of Panc-1 cells. Cells were then exposed to increasing concentration of pimoziide or DMSO for 10 hours until the gap closed in the DMSO control. The size of the wound gap at 10 hours was compared with the size at time zero for each drug concentration. (B) Consistent with inhibition of cell migration, pimoziide treatment increased E-cadherin and decreased vimentin protein levels in a dose-dependent manner in Panc-1 cells. (C) The dose-dependent inhibitory effects of pimoziide and L741 on the migration of MiaPaCa-2 cells. Cells were plated on Transwells (Boyden chamber) and migrated cells were counted and normalized to controls after exposure to different doses of pimoziide or L-741 for 4 hours. (D) Inhibition of cAMP/PKA rescued the inhibitory effect of DRD2 blockade on the migration of Panc-1 cells. Cells were plated on Transwells and exposed to L-741 (*left*) or pimoziide (*right*) for 4 hours in the presence or absence of H89 or SQ22536, and cell migration assayed as described in (C). Values are the mean of 4 replicate experiments. * $P < .05$ and ** $P < .01$ when compared with the corresponding results at 0 μM (Mann-Whitney U test).

migration was specific for the 2-dimensional wound healing assay, we examined the migration of Panc-1 cells by the quantitative 3-dimensional Boyden chamber assay in the presence of pimoziide, which confirmed that the treatment suppresses cell migration (Supplementary Figure 4C). Furthermore, we validated the inhibitory effect of pimoziide and L-741 on pancreatic cancer cell migration by testing another cell line (MiaPaCa-2) (Figure 5C). In order to verify the involvement of the cAMP/PKA pathway in the observed inhibitory effect of DRD2 blockade, we analyzed cell migration while perturbing this pathway. The reduction in cell migration upon treatment with pimoziide or L-741 was rescued by the addition of H89 or SQ22536, which both reduce PKA activation and cAMP levels (Figure 5D, and Supplementary Figure 4D). Taken together, these results demonstrated that the DRD2 blockade suppresses pancreatic cancer cell migration by induction of cAMP and activation of PKA.

Blockade of Dopamine Receptor D2 Reduces Tumor Growth and Metastasis in Vivo

We replicated anti-cancer effects of DRD2 inhibition using another FDA-approved DRD2 antagonist haloperidol.²⁸ Haloperidol treatment showed the same effects as those observed with pimoziide and L-741 treatments (Figure 6A–E). Interestingly, however, haloperidol displayed

the lowest toxicity on normal fibroblast cells among DRD2 inhibitors examined in our study. Therefore, we set out to verify the anti-cancer effects of haloperidol in orthotopic models of pancreatic cancer, which we generated by implanting MiaPaCa-2 cells into the tail of the pancreas of Nod scid gamma mice. After tumor development, mice were randomized into 2 groups and treated with haloperidol ($n = 9$) or control solvent ($n = 7$). Haloperidol treatment (10 mg/kg selected based on results reported for glioblastoma treatment²⁹) reduced tumor volume, weight, and metastatic dissemination significantly ($P < .001$), while showing no significant effect on animal weight (Figure 6F).

Discussion

Investigating novel targeted therapeutic opportunities for PDAC, we applied a combination of pathway- and network-based approaches to PDAC transcriptome profiles. Specifically, we leveraged on identifying aberration hubs by overlaying PDAC-associated gene expression patterns on the human protein interaction network in order to highlight factors with potential driver activities among the plethora of deregulated genes. This led to the identification of DRD2, which we validated as a novel promising therapeutic target. Our findings revealed a high expression of DRD2 in PDAC, and confirmed the efficacy of its blockade to suppress cancer cell proliferation, survival, and metastasis potential.

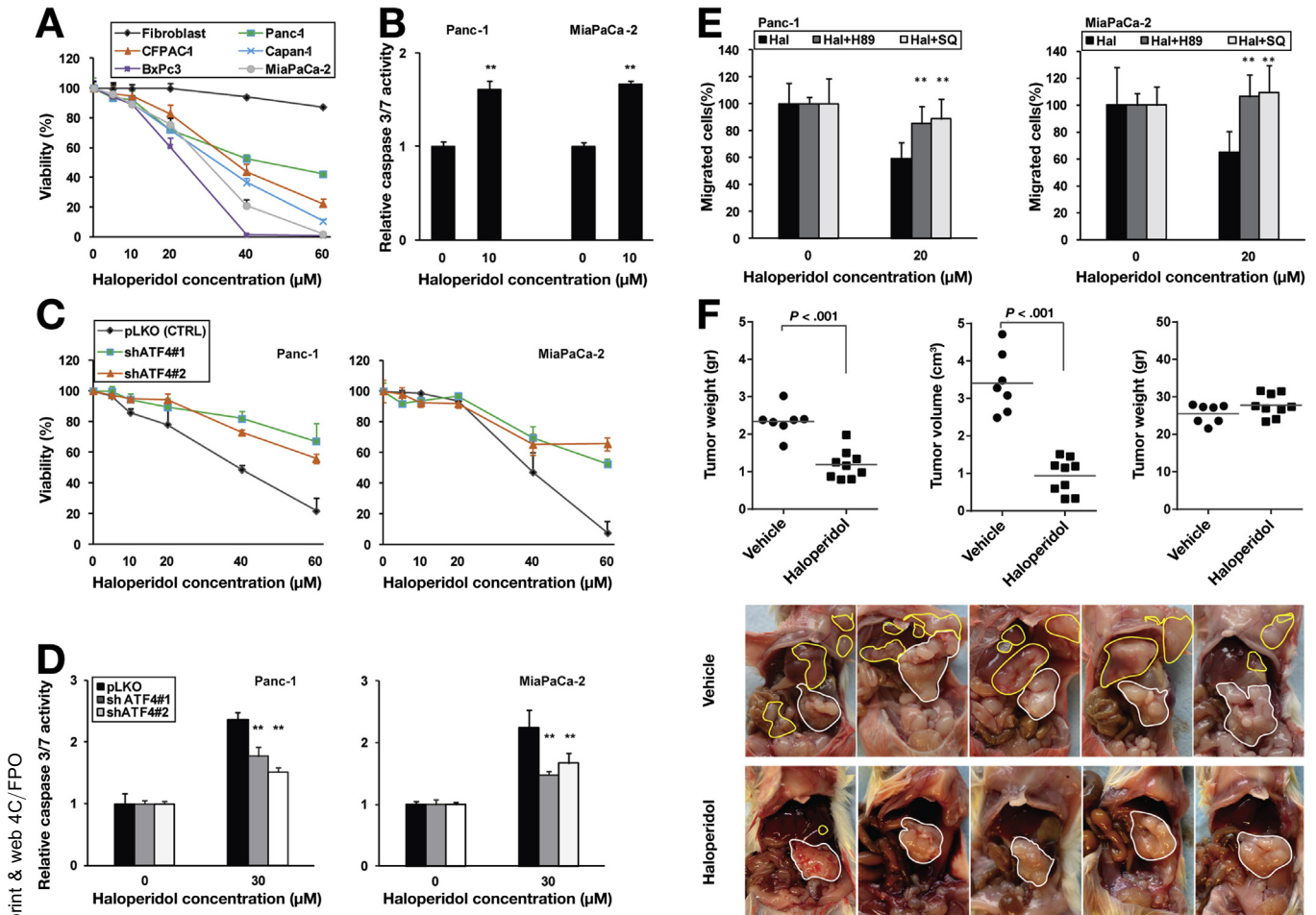


Figure 6. Anti-cancer effects of haloperidol. (A) Dose-dependent anti-proliferative effects of haloperidol on pancreatic cancer cells assayed by sulforhodamine B assay 72 hours post-treatment. (B) Induction of apoptosis by haloperidol as measured by assaying caspase 3/7 activation 24 hours after treatment. Inhibition of ER stress-UPR activation through ATF4 knockdown rescues, at least in part, the anti-proliferative (C) and apoptosis-inducing (D) effects of haloperidol on Panc-1 and MiaPaCa-2 cells. (E) Inhibition of cAMP/PKA rescued the inhibitory effect of haloperidol (Hal) on the migration of Panc-1 (left) and MiaPaCa-2 (right) cells. (F) Treatment with haloperidol reduces tumor volume and metastasis burden in vivo. MiaPaCa-2 cells (2×10^6) were orthotopically injected into the tail of the pancreas of NSG mice. Twenty-seven days post-surgery, mice were randomized into 2 groups and treated with either haloperidol (10 mg/kg, intraperitoneal) or vehicle for 12 days. The experiment was terminated when control animals became moribund. Animal weight, tumor weight, and tumor volume were measured at time of sacrifice. *Upper panel:* Tumor weight (left) and volume (middle) were significantly reduced in mice treated with haloperidol compared with the control group, while there was no significant change in body weight (right) between groups. *Bottom panel:* Representative images show tumors in mice. *White and yellow outlines* show primary and metastatic tumors, respectively. Treatment with haloperidol reduced the metastasis dissemination. $**P < .01$ when compared with the corresponding results at 0 μM in (B), pLKO at 30 μM in (D) or haloperidol at 20 μM in (E) (Mann-Whitney U test).

We found that DRD2 blockade has an anti-proliferative effect in pancreatic cancers, while activating ER stress, in line with previous studies reporting that the deficiency of DRD2 induces ER stress.¹⁵ The accelerated proliferation of cancer cells in solid tumors often leads to nutrient deprivation in their microenvironment and results in protein misfolding, which eventually triggers activation of ER stress.¹⁶ Whereas moderate ER stress supports cell survival in nutrient-deprived conditions, excessive ER stress leads to cell cycle arrest and apoptosis,^{30,31} and has emerged as an attractive anti-cancer therapeutic avenue.^{32,33} As such, inhibiting DRD2 provides a targeted approach to activate ER stress in cancer cells.

Importantly, when compared with normal samples, DRD2 expression was elevated significantly in CP, which is a known major risk factor for PDAC,¹¹ suggesting that DRD2 overexpression may be involved in the early steps of PDAC development. In line with this observation, Sachlos and colleagues³⁴ have shown that dopamine receptors are overexpressed in human cancer stem cells and that inhibition of dopamine receptor signaling can serve as an effective approach to impair tumorigenicity of cancer stem cells. Notably, both studies utilized DRD2 antagonists that are approved by the FDA as antipsychotic agents (pimozide and haloperidol in our study and thioridazine in Sachlos et al). Interestingly, schizophrenic patients receiving DRD2

antagonists have a reduced incidence rate of different solid tumors, including those of rectum, colon, and prostate, compared with the general population.³⁵ Likewise, lower cancer incidence rates have been reported in patients suffering from Parkinson's disease in which the dopaminergic pathway is deficient.³⁶ These findings suggest that dopaminergic signaling may be involved in the development of multiple cancers, and may potentially serve as a pan-cancer therapeutic target. Supporting this, DRD2 antagonists have also shown anti-cancer effects in leukemia³⁴ and glioblastoma.²⁹ However, other effectors including signal transducer and activator of transcription 5 and extracellular signal-regulated kinase signaling have been proposed as mediators of DRD2 function in these tumors. Notably, we did not observe a decrease in phosphorylation of signal transducer and activator of transcription 5 or extracellular signal-regulated kinase in PDAC cells upon treatment with DRD2 antagonists (Supplementary Figure 5), but validated that the anti-growth effect of pimozone and haloperidol on pancreatic cancer cells is primarily through targeting DRD2 (Supplementary Figure 6). Given the inherent heterogeneous nature of cancer and the involvement of GPCRs in multiple signaling cascades,⁸ it is possible that the functional consequences of DRD2 blockade are mediated through various signaling pathways in different tumors. Additional experiments are warranted to elucidate the exact mechanism of DRD2 inhibition in pancreatic cancer.

Our study highlights the potential of DRD2 antagonism as a possible therapeutic approach in pancreatic cancer, which could be facilitated through a drug-repositioning strategy, as previously practiced for pimozone in treatment of metastatic melanoma.³⁷ This also motivates future studies to investigate possible relationships between DRD2 levels and different PDAC subtypes, emerged by transcriptome³⁸ and metabolite profiling,³⁹ which may lead to a better understanding of DRD2 function in PDAC, and help with tailoring therapy for individual patients.

Supplementary Material

Note: To access the supplementary material accompanying this article, visit the online version of *Gastroenterology* at www.gastrojournal.org, and at <http://dx.doi.org/10.1053/j.gastro.2016.08.040>.

References

1. Siegel RL, Miller KD, Jemal A. Cancer statistics, 2015. *CA Cancer J Clin* 2015;65:5–29.
2. Costello E, Greenhalf W, Neoptolemos JP. New biomarkers and targets in pancreatic cancer and their application to treatment. *Nat Rev Gastroenterol Hepatol* 2012;9:435–444.
3. Trouilloud I, Dubreuil O, Boussaha T, et al. Medical treatment of pancreatic cancer: new hopes after 10 years of gemcitabine. *Clin Res Hepatol Gastroenterol* 2011;35:364–374.
4. Kim MP, Gallick GE. Gemcitabine resistance in pancreatic cancer: picking the key players. *Clin Cancer Res* 2008;14:1284–1285.
5. de Souza Rocha Simonini P, Breiling A, Gupta N, et al. Epigenetically deregulated microRNA-375 is involved in a positive feedback loop with estrogen receptor alpha in breast cancer cells. *Cancer Res* 2010;70:9175–9184.
6. Kanehisa M, Goto S. KEGG: kyoto encyclopedia of genes and genomes. *Nucleic Acids Res* 2000;28:27–30.
7. Gold MG, Gonen T, Scott JD. Local cAMP signaling in disease at a glance. *J Cell Sci* 2013;126:4537–4543.
8. Neves SR, Ram PT, Iyengar R. G protein pathways. *Science* 2002;296:1636–1639.
9. Menche J, Sharma A, Kitsak M, et al. Disease networks. Uncovering disease-disease relationships through the incomplete interactome. *Science* 2015;347:1257601.
10. Zimmerman NP, Roy I, Hauser AD, et al. Cyclic AMP regulates the migration and invasion potential of human pancreatic cancer cells. *Mol Carcinog* 2015;54:203–215.
11. Bang UC, Benfield T, Hyldstrup L, et al. Mortality, cancer, and comorbidities associated with chronic pancreatitis: a Danish nationwide matched-cohort study. *Gastroenterology* 2014;146:989–994.
12. Scholzen T, Gerdes J. The Ki-67 protein: from the known and the unknown. *J Cell Physiol* 2000;182:311–322.
13. Mothi M, Sampson S. Pimozone for schizophrenia or related psychoses. *Cochrane Database Syst Rev* 2013;11:CD001949.
14. Bowery BJ, Razzaque Z, Emms F, et al. Antagonism of the effects of (+)-PD 128907 on midbrain dopamine neurones in rat brain slices by a selective D2 receptor antagonist L-741,626. *Br J Pharmacol* 1996;119:1491–1497.
15. Tinsley RB, Bye CR, Parish CL, et al. Dopamine D2 receptor knockout mice develop features of Parkinson disease. *Ann Neurol* 2009;66:472–484.
16. Clarke HJ, Chambers JE, Liniker E, et al. Endoplasmic reticulum stress in malignancy. *Cancer Cell* 2014;25:563–573.
17. Stutzmann GE, Mattson MP. Endoplasmic reticulum Ca(2+) handling in excitable cells in health and disease. *Pharmacol Rev* 2011;63:700–727.
18. Tovey SC, Dedos SG, Rahman T, et al. Regulation of inositol 1,4,5-trisphosphate receptors by cAMP independent of cAMP-dependent protein kinase. *J Biol Chem* 2010;285:12979–12989.
19. Holz GG, Leech CA, Heller RS, et al. cAMP-dependent mobilization of intracellular Ca²⁺ stores by activation of ryanodine receptors in pancreatic beta-cells. A Ca²⁺ signaling system stimulated by the insulinotropic hormone glucagon-like peptide-1-(7-37). *J Biol Chem* 1999;274:14147–14156.
20. Li L, Miyamoto M, Ebihara Y, et al. DRD2/DARPP-32 expression correlates with lymph node metastasis and tumor progression in patients with esophageal squamous cell carcinoma. *World J Surg* 2006;30:1672–1679; discussion 1680–1681.
21. Davies SP, Reddy H, Caivano M, et al. Specificity and mechanism of action of some commonly used protein kinase inhibitors. *Biochem J* 2000;351:95–105.

- 1441 22. Freyberg Z, Ferrando SJ, Javitch JA. Roles of the Akt/
1442 GSK-3 and Wnt signaling pathways in schizophrenia
1443 and antipsychotic drug action. *Am J Psychiatry* 2010;
1444 167:388–396.
- 1445 23. Arguello PA, Gogos JA. A signaling pathway AKTing up
1446 in schizophrenia. *J Clin Invest* 2008;118:2018–2021.
- 1447 24. **Hamanaka RB, Bennett BS**, Cullinan SB, et al. PERK
1448 and GCN2 contribute to eIF2alpha phosphorylation and
1449 cell cycle arrest after activation of the unfolded protein
1450 response pathway. *Mol Biol Cell* 2005;16:5493–5501.
- 1451 25. Brewer JW, Hendershot LM, Sherr CJ, et al. Mammalian
1452 unfolded protein response inhibits cyclin D1 translation
1453 and cell-cycle progression. *Proc Natl Acad Sci U S A*
1454 1999;96:8505–8510.
- 1455 26. Maly DJ, Papa FR. Druggable sensors of the unfolded
1456 protein response. *Nat Chem Biol* 2014;10:892–901.
- 1457 27. Lytton J, Westlin M, Hanley MR. Thapsigargin inhibits the
1458 sarcoplasmic or endoplasmic reticulum Ca-ATPase
1459 family of calcium pumps. *J Biol Chem* 1991;266:
1460 17067–1771.
- 1461 28. Granger B, Albu S. The haloperidol story. *Ann Clin Psy-*
1462 *chiatry* 2005;17:137–140.
- 1463 29. Li J, Zhu S, Kozono D, et al. Genome-wide shRNA screen
1464 revealed integrated mitogenic signaling between dopa-
1465 mine receptor D2 (DRD2) and epidermal growth factor
1466 receptor (EGFR) in glioblastoma. *Oncotarget* 2014;
1467 5:882–893.
- 1468 30. Yang ZJ, Chee CE, Huang S, et al. The role of autophagy
1469 in cancer: therapeutic implications. *Mol Cancer Ther*
1470 2011;10:1533–1541.
- 1471 31. Mollereau B. Establishing links between endoplasmic
1472 reticulum-mediated hormesis and cancer. *Mol Cell Biol*
1473 2013;33:2372–2374.
- 1474 32. Li X, Zhang K, Li Z. Unfolded protein response in cancer:
1475 the physician's perspective. *J Hematol Oncol* 2011;4:8.
- 1476 33. Liu Y, Ye Y. Proteostasis regulation at the endoplasmic
1477 reticulum: a new perturbation site for targeted cancer
1478 therapy. *Cell Res* 2011;21:867–883.
- 1479 34. Sachlos E, Risueno RM, Laronde S, et al. Identification of
1480 drugs including a dopamine receptor antagonist that selec-
1481 tively target cancer stem cells. *Cell* 2012;149:1284–1297.
- 1482 35. Dalton SO, Mellekjaer L, Thomassen L, et al. Risk for
1483 cancer in a cohort of patients hospitalized for schizo-
1484 phrenia in Denmark, 1969–1993. *Schizophr Res* 2005;
1485 75:315–324.
- 1486 36. Driver JA, Logroscino G, Buring JE, et al. A prospective
1487 cohort study of cancer incidence following the diagnosis
1488 of Parkinson's disease. *Cancer Epidemiol Biomarkers*
1489 *Prev* 2007;16:1260–1265.
- 1490 37. Neifeld JP, Tormey DC, Baker MA, et al. Phase II trial of
1491 the dopaminergic inhibitor pimozide in previously treated
1492 melanoma patients. *Cancer Treat Rep* 1983;67:155–157.
- 1493 38. Collisson EA, Sadanandam A, Olson P, et al. Subtypes of
1494 pancreatic ductal adenocarcinoma and their differing
1495 responses to therapy. *Nat Med* 2011;17:500–503.
- 1496 39. Daemen A, Peterson D, Sahu N, et al. Metabolite profiling
1497 stratifies pancreatic ductal adenocarcinomas into sub-
1498 types with distinct sensitivities to metabolic inhibitors.
1499 *Proc Natl Acad Sci U S A* 2015;112:E4410–E4417.

Author names in bold designate shared co-first authorship.

Received September 4, 2015. Accepted August 4, 2016.

Reprint requests

Address requests for reprints to: Yasser Riazalhosseini, XX, Department of Human Genetics, McGill University and Genomic Quebec Innovation Centre, 740 Dr Penfield Avenue, Room 4203, Montreal Quebec H3A 0G1, Canada. e-mail: Yasser.riazalhosseini@mcgill.ca; fax: (514) 398-3955.

Acknowledgments

The authors are grateful to Sebastian Perner, Rita Viciunaite, Brunhilde Bentzinger, and Shabnam Assadinia for technical assistance.

Hamed S. Najafabadi, Andrea S. Bauer, and Andreas I. Papadakis contributed equally to this work. Yasser Riazalhosseini and Jörg D. Hoheisel supervised the study jointly.

Accession Code of microarray dataset: The complete dataset deposited in the public ArrayExpress database (<http://www.ebi.ac.uk/arrayexpress/>) under accession code E-MTAB-1791.

Conflicts of interest

These authors disclose the following: Pouria Jandaghi, Jörg D. Hoheisel, and Yasser Riazalhosseini filed for patent protection for the application of DRD2 antagonists as therapeutic agents against pancreatic cancer. The remaining authors disclose no conflicts.

Funding

This work was supported financially by a grant to Jörg D. Hoheisel of the German Federal Ministry of Education and Research (BMBF) as part of grant no. 01GS08117 within the PaCaNet consortium. Collection of the samples in Heidelberg was performed by the EPZ-PancoBank (MWK), which is supported by the Heidelberger Stiftung Chirurgie and the BMBF grants 01GS08114, 01ZX1305C, and 01EY1101. Also, support to Jörg D. Hoheisel through the Integrated European Platform for Pancreas Cancer Research (COST Action no. BM1204) is gratefully acknowledged. This work has also been supported in part by a grant from Canadian institutes of Health Research (CIHR; TFC-145428) to Yasser Riazalhosseini, and a grant from the Ministère de l'économie, de l'innovation et de l'exportation du Québec through Génome Québec to Mark Lathrop. Sidong Huang is recipient of a Canada Research Chair in Functional Genomics and also a CIHR grant (MOP no. 130540); Andreas I. Papadakis is recipient of a CIHR-funded McGill Chemical Biology Postdoctoral Fellowship. Aldo Scarpa is supported by the Italian Association for Cancer Research (AIRC 5x1000 grant no. 12182), Cam-Pac FP7 (grant agreement no. 602783), and the Italian Cancer Genome Project (FIRB RBAP10AHJB). George Zogopoulos is a clinical research scholar of the Fonds de Recherche du Québec-Santé (FRQS).

1501
1502
1503
1504
1505
1506
1507
1508
1509
1510
1511
1512
1513
1514
1515
1516
1517
1518
1519
1520
1521
1522
1523
1524
1525
1526
1527
1528
1529
1530
1531
1532
1533
1534
1535
1536
1545
1546
1547
1548
1549
1550
1551
1552
1553
1554
1555
1556
1557
1558
1559
1560